Laser Spectroscopy of the Fine-Structure Splitting in the 2^3P_J Levels of ^{4}He

X. Zheng,[1] Y. R. Sun,[1,2,*] J.-J. Chen,[1] W. Jiang,[3] K. Pachucki,[4] and S.-M. Hu[1,†]
[1]Hefei National Laboratory for Physical Sciences at the Microscale, iChem Center, University of Science and Technology of China, Hefei 230026, China
[2]Synergetic Innovation Center of Quantum Information and Quantum Physics, University of Science and Technology of China, Hefei 230026, China
[3]School of Nuclear Science and Technology, University of Science and Technology of China, Hefei 230026, China
[4]Faculty of Physics, University of Warsaw, Pasteura 5, 02-093 Warsaw, Poland
(Received 13 December 2016; published 10 February 2017)

The fine-structure splitting in the 2^3P_J ($J = 0, 1, 2$) levels of ^{4}He is of great interest for tests of quantum electrodynamics and for the determination of the fine-structure constant α. The 2^3P_0-2^3P_2 and 2^3P_1-2^3P_2 intervals are measured by laser spectroscopy of the ^3P_J-2^3S_1 transitions at 1083 nm in an atomic beam, and are determined to be $31\,908\,130.98 \pm 0.13$ kHz and $2\,291\,177.56 \pm 0.19$ kHz, respectively. Compared with calculations, which include terms up to α^5Ry, the deviation for the α-sensitive interval 2^3P_0-2^3P_2 is only 0.22 kHz. It opens the window for further improvement of theoretical predictions and an independent determination of the fine-structure constant α with a precision of 2×10^{-9}.

DOI: 10.1103/PhysRevLett.118.063001

As the simplest multielectron system, atomic helium has played an important role in the history of quantum electrodynamics (QED) through increasingly refined comparisons between experimental data and theoretical predictions. The fine structure of the 2^3P_J ($J = 0, 1, 2$) levels of ^{4}He, with a large splitting interval of 31.9 GHz, was recognized [1] as the best atomic system for the determination of the fine-structure constant α. It is also the best system for studying exotic spin-dependent interactions between electrons [2], as it is presently more sensitive than the positronium atom. The reasons include the relatively long lifetime of the 2^3P_J levels in the helium atom, as compared to those in the hydrogen atom, and the weak dependence on the finite nuclear size, which usually limits the accuracy of theoretical predictions. In the past 50 years, the helium fine structure has been calculated with unprecedented precision by gradually including terms up to the order of α^5Ry [3–5]. Although at present it is calculated with the highest precision among all the multielectron atoms, the α value determined from the 2^3P_J fine structure of ^{4}He is less accurate than those from the electron magnetic moment anomaly [6] and atomic recoil [7].

Considerable efforts have been made by both theorists and experimentalists in the last few decades, but there are still disagreements among the reported results. The latest theoretical work by Pachucki *et al.* [5] gives an uncertainty of 1.7 kHz for both splitting intervals 2^3P_0-2^3P_2 (ν_{02}) and $2^3P_1 - 2^3P_2$ (ν_{12}). As shown in Fig. 1, the experimental results for the ν_{12} interval from different groups [8–11] used to show obvious discrepancies even within the stated uncertainties. These have recently been resolved by taking into account the quantum interference corrections [12], which had not been considered in previous measurements. As for the ν_{02} interval of 31.9 GHz, it has been measured by several groups employing a variety of methods, including direct microwave spectroscopy with a thermal atomic beam [13], saturation absorption spectroscopy in a discharge cell [10], and laser spectroscopy with a thermal atomic beam [14]. As shown in Fig. 1, there are apparent disagreements among the experimental and theoretical values. Prior to this work, the most precise experimental measurement was given by Smiciklas and Shiner [14] as 31 908 131.25 kHz with an uncertainty of 0.3 kHz. However, the microwave and saturation absorption spectroscopy values differ from this value by 2.7 kHz (1.5σ) and 4.5 kHz (4.5σ), respectively. Note that this discrepancy cannot be accounted for by the quantum interference correction, which is pronounced for the ν_{12} interval but much less so for the ν_{02} interval. Therefore, more independent measurements are required.

In this Letter we present the most accurate experimental determination of the ν_{02} and ν_{12} intervals to date using laser spectroscopy of ^{4}He atoms. By using an intense atomic beam transversely cooled by a resonant laser field, the signal-to-noise ratio of the recorded spectrum is improved and the uncertainty of the determined ν_{02} interval is reduced to 0.13 kHz. This would allow an independent determination of the fine-structure constant α with a precision of about 2×10^{-9}, provided theoretical predictions reach a similar level of accuracy.

The experimental setup consists of two parts: an atomic beam line and an optical bench, as shown in Fig. 2. The configuration of the atomic beam line is similar to that reported in our previous work [8]. Helium atoms at the 2^3S_1 metastable state are first produced by radio-frequency discharge and then collimated by transverse cooling with

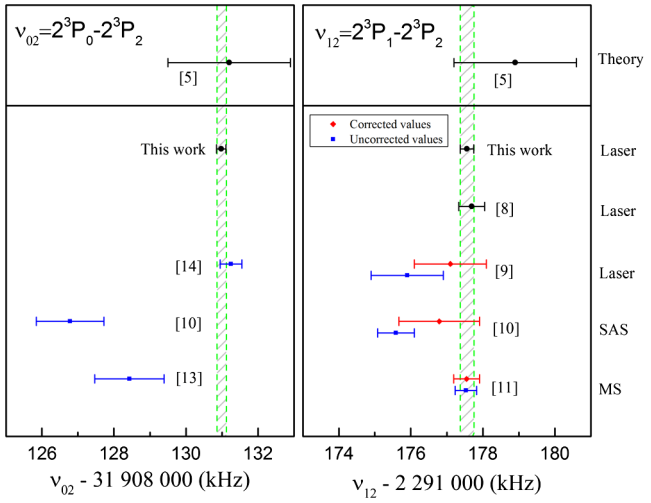

FIG. 1. Comparison of the ν_{02} and ν_{12} values from experimental and theoretical studies. The results for the ν_{12} values are shown with (red) and without (blue) quantum interference corrections. The correction is much less for ν_{02} and is not shown here. The corresponding methods are listed on the right side: laser spectroscopy with atomic beam (Laser), saturation absorption spectroscopy (SAS) in discharge cell, and microwave spectroscopy (MS) with atomic beam.

a laser on resonance with the 2^3S_1-2^3P_2 transition. A two-dimensional magneto-optical trap is used to slightly focus the atomic beam and a second transverse cooling field deflects the atoms at the triplet state (2^3S_1-2^3S_1) from the original atomic beam by an angle of 0.1° to eliminate the background of unwanted particles such as singlet state (2^1S_0) atoms and UV photons [15–17]. A circularly polarized laser beam is applied to pump the atoms from the 2^3S_1 ($m=0$) level to 2^3P_1. After several cycles of excitation and spontaneous decay, over 99% of the atoms at the 2^3S_1 ($m=0$) state are transferred to the 2^3S_1 ($m=+1$) state (or $m=-1$, depending on the pump laser's polarization). The atoms then enter the spectral probe region where the 2^3S_1 ($m=0$) state is repopulated by the probe laser scanning through the resonance of the ^3P_J-2^3S_1 ($J=0,\ 2$) transition. This region is shielded with three layers of cylinder-shaped μ metal, inside which a homogeneous magnetic field is generated by a $\cos(\theta)$ coil. A Stern-Gerlach magnet is used to deflect the atoms at $m=\pm1$ levels so that only atoms in the $m=0$ level can reach the detector at the end of the beam line. Owing to an enhanced atomic beam intensity, the signal-to-noise ratio has been improved by a factor of 5 compared with our previous study [8].

A full beat-lock laser chain and a sideband-free probing system are used for spectroscopy in this work, which is quite different from that used in our previous study [8]. A narrow-band fiber laser (NKT Photonics Koheras BOOSTIK Y10, referred to as the master laser), with a linewidth of 10 kHz, is locked to a longitudinal mode of a temperature-stabilized Fabry-Pérot cavity made of ultralow expansion glass [18,19]. An external-cavity diode laser (referred to as the cooling laser) with its frequency tuned to the 2^3P_2-2^3S_1 transition is used for transverse cooling. A distributed feedback laser, referred to as the pump laser, with its frequency tuned on resonance with the 2^3P_1-2^3S_1 transition is used for optical pumping. A fiber EOM is used to produce $\pm1^{st}$ sidebands of up to 16 GHz on the master laser frequency. The fiber EOM is driven by a rf synthesizer (R&S SMB100A) referenced to a rubidium clock (Spectratime GPS Reference-2000). Two external-cavity diode lasers (ECDL1 and ECDL2, referred to as probe lasers) are phase locked to the $+1^{st}$ and -1^{st} sidebands respectively [see Fig. 2(c)], whose frequency can be fine-tuned near the transition resonances (2^3P_2-2^3S_1 and 2^3P_0-2^3S_1). Both beams from ECDL1 and ECDL2 are coupled into one single-mode optical fiber after a beam splitter. Two mechanical shutters (EOPC CH-60) are used for time-sequence control of the two probe lasers so that during each data acquisition cycle there is only one probe laser interacting with the atomic beam. A frequency scan covers the 2^3P_2-2^3S_1 and 2^3P_0-2^3S_1 transitions successively by switching between the two probe lasers, with 22 frequency points around each peak. The scan sequence is purposely randomized to avoid possible systematic shifts due to the frequency drift of the master laser.

The laser system in our previous study [8] was similar to that used by Smiciklas and Shiner [14] in that the carrier laser and both sidebands interacted with the atomic beam in the probe region. Although only one sideband scanned though the resonance, there was still concern that the presence of the carrier and the other sideband could cause a systematic deviation. In this study we avoided the potential influence from sidebands by selecting only one beam (with no sidebands) into the probe region. Another advantage of present configuration is that the probe laser

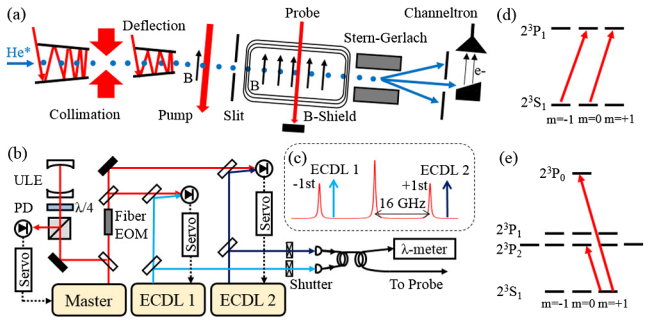

FIG. 2. (a) The configuration of the experimental setup. (b) Optical layout: acoustic-optic modulator (AOM), external-cavity diode laser (ECDL), electro-optic modulator (EOM), photodiode (PD), and Fabry-Pérot interferometer made of ultra-low-expansion (ULE) glass. (c) Diagram of the frequency intervals between the master laser and two ECDL lasers. (d) Transitions excited by the pump laser. (e) Transitions excited by the probe laser.

power can be stabilized with considerably better precision, which also eliminates the uncertainty due to variations of the fiber EOM sideband power.

In total, we carried out about 7000 scans of the transitions 2^3P_2-2^3S_1 and 2^3P_0-2^3S_1. The spectra were used to derive the frequency interval ν_{02}, for which a statistical uncertainty of 0.06 kHz is obtained. Various systematic effects have been investigated, described below.

Power dependence.—There is a dependence of the measured frequency interval on the power of the probe laser, which is a result of the recoil-induced Doppler shift. Under each experimental condition, a series of measurements were carried out with different probe laser powers in the range of 1/20 to 1/4 of the transition saturation intensity (167 μW/cm^2). The frequency interval obtained is found to be linear with the laser power within this range. Measurements both with and without retroreflected probe laser beam have been carried out. We also repeated measurements using both initial states ($m = +1$ and $m = -1$). As shown in Fig. 3, the same result is obtained when we extrapolate different groups of data to the zero-laser-power limit. When the laser power is lower than 1/4 of the saturation intensity, the contribution to the uncertainty from the power dependence is expected to be less than 60 Hz.

Zeeman shift.—The first-order Zeeman shift cancels for the 2^3P_0-2^3P_2 ($m = 0$) interval and the second-order Zeeman shift can be calculated using the coefficient given by Yan and Drake [20]. In this work, a magnetic field bias of 10 to 20 G was applied; the ν_{02} values obtained are shown in Fig. 4(a). The magnetic field intensity was determined with an accuracy better than 2 mG by measuring the frequency interval between the $m = +1$ and $m = -1$ states of the 2^3S_1 level. The second-order Zeeman shifts have been included in each frequency difference value. The resulting contribution to the uncertainty in the zero-field ν_{02} value is less than 60 Hz. The contribution due to the residual magnetic field (<0.3 mG) in the probe region is below 10 Hz and therefore neglected.

Doppler shift.—The Doppler shift arises if the laser beam is not exactly perpendicular to the atomic beam. We can observe the misalignment by monitoring the separation between two peaks of one transition produced by a retroreflected laser beam. In this way, we confirm that the misalignment in our experiments is less than ± 5 μrad, corresponding to a separation of 5 kHz. Because the conditions are the same during the measurement of both the 2^3P_2-2^3S_1 and the 2^3P_0-2^3S_1 transitions, the influence on the frequency interval ν_{02} due to the Doppler shift is further reduced. We have purposely misaligned the laser beam to investigate this effect. The deviation observed in the ν_{02} interval is below 500 Hz even with a misalignment of 200 μrad. We estimate that the deviation should be less than 25 Hz when the misalignment is within 10 μrad.

Quantum interference.—According to Marsman *et al.* [21] and the experimental studies on the transition frequency of lithium [22,23] and ytterbium [24], a quantum interference effect should be taken into account. A correction of +1.21 kHz has been included in the frequency interval ν_{12} (2^3P_1-2^3P_2) obtained in our study [8]. In the case of the interval ν_{02}, which is about 14 times larger than ν_{12}, the correction is much smaller. In addition, because the $2^3P_1(m = 0)$-$2^3S_1(m = 0)$ transition is dipole forbidden, the interference shift due to the 2^3P_1 state is eliminated. We carried out a calculation of this interference effect under our experimental conditions and found that the correction for the ν_{02} interval is $+0.08 \pm 0.03$ kHz.

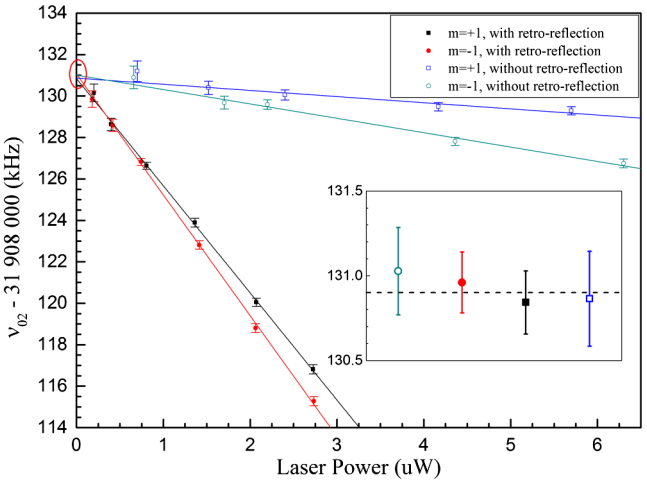

FIG. 3. Dependence of the measured frequency interval on the probe laser power. The inset shows the values extrapolated to the zero-laser-power limit. The plot shows measurements for the initial state $m = +1$ with retroreflection (solid squares), $m = -1$ with retroreflection (solid circles), $m = +1$ without retroreflection (open squares), and $m = -1$ without retroreflection (open circles).

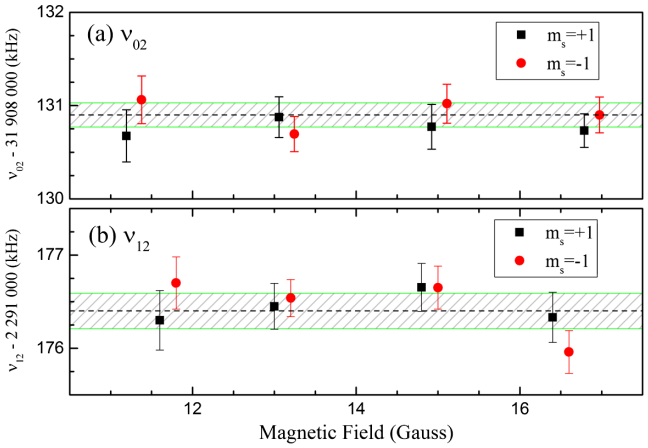

FIG. 4. The (a) 2^3P_0-2^3P_2 splitting ν_{02} and (b) 2^3P_1-2^3P_2 splitting ν_{12} obtained at different magnetic fields. The values are corrected with the calculated second-order Zeeman shifts. The squares and circles represent the transitions measured from different initial states with $m = +1$ and $m = -1$, respectively.

Other systematic effects.—We have also investigated other factors that may potentially introduce systematic shifts, including the following.

(i) ac Stark shift due to scattering light from the strong laser beams used for optical pumping. We did not observe any difference when using half the pump power.

(ii) Probe laser polarization. The laser is circularly polarized and propagates in the direction parallel to the magnetic field bias. However, if the alignment is imperfect, the atoms could experience linear polarization components and be excited to the other magnetic sublevels ($m = +1$ or $m = -1$) for the 2^3P_2-2^3S_1 transition, which could possibly introduce an asymmetry in the spectral line profile. We investigated this effect by using a linear polarized laser beam (instead of circular one) in the measurement, but we still could not observe any significant shift. Taking into account that the circular polarization purity of the probe laser is better than 30:1, we estimate that the resulted frequency shift due to imperfect polarization of the probe beam should be less than 30 Hz.

(iii) Difference between the two probe lasers (ECDL1 and ECDL2) used in the experiment. These two lasers are phase-locked to $\pm 1^{\text{st}}$ sidebands of the master laser, respectively. In order to check the consistency of the results, we swapped the roles of these two probe lasers and measured the same transition. The center frequencies obtained from both lasers agree with each other.

(iv) Deviation between the results from different initial states ($m = +1$ or $m = -1$). The experimental results obtained from both initial states agree within the stated uncertainty of the present study.

(v) The atomic density at the probe region is about 10^8 cm^{-3} and the collision effect is negligible.

The overall uncertainty budget is given in Table I. The statistical uncertainty is 0.06 kHz for the ν_{02} value obtained in the present work. Taking into account the various effects discussed above, the systematic uncertainty is estimated to be 0.11 kHz in total. As a result, the ν_{02} value is determined to be $31\,908\,130.98 \pm 0.06(\text{stat}) \pm 0.11(\text{syst})$ kHz. As shown in Fig. 1, this value agrees well with the most recent laser spectroscopy study in a thermal atomic beam by Smiciklas and Shiner (0.27 ± 0.30 kHz) [14], but differs by 4.20 ± 0.94 kHz (4σ) from that of the saturation absorption spectroscopy [10], and also by 2.55 ± 0.96 kHz (2.6σ) from that of the microwave spectroscopy [11,13]. The present result agrees with the most recent theoretical result taking into account all the QED effects up to the order of α^5Ry [5]. The difference between the theoretical and experimental ν_{02} values is $0.22 \pm 0.13_{\text{exp}} \pm 1.7_{\text{theo}}$ kHz.

TABLE I. Uncertainty budget (in kHz).

Source	ν_{02}	$\Delta\nu(1\sigma)$	ν_{12}	$\Delta\nu(1\sigma)$
Statistical	31 908 130.90	0.06	2 291 176.35	0.08
Zeeman effect		0.06		0.09
Laser power		0.06		0.06
First-order Doppler		0.03		0.03
Stray light		0.02		0.02
Laser polarization		0.03		0.08
Initial states		0.04		0.04
Quantum interference	+0.08	0.03	+1.21	0.10
Total	31 908 130.98	0.13	2 291 177.56	0.19

The 2^3P_1-2^3P_2 interval (ν_{12}) has been determined in our previous study [8] and is measured again using the present apparatus. Part of the results are shown in Fig. 4(b). Compared to our previous result, the statistical uncertainty in the present work has been reduced to 0.08 kHz. Because the experimental conditions have also been better controlled, the quantum interference effect contributed to the ν_{12} interval is evaluated with an uncertainty of 0.10 kHz. The contributions to the uncertainty from the power drift due to fiber-EOM sidebands is eliminated because a different spectral scanning scheme is used here. The new value for ν_{12} is determined to be $2\,291\,177.56 \pm 0.08(\text{stat}) \pm 0.18(\text{syst})$ kHz, agreeing very well with our previous value $2\,291\,177.69 \pm 0.36$ kHz [8]. Note that the experimental conditions are quite different between our previous study and the present one. This good agreement shows the excellent reproducibility of our measurements. The difference between the theoretical and experimental ν_{12} values is $1.5 \pm 0.19_{\text{exp}} \pm 1.7_{\text{theo}}$ kHz.

The very good agreement between theoretical predictions and our experimental result for the 2^3P_0-2^3P_2 interval is the first, and so far the only, confirmation of the correctness of the calculation of α^5Ry QED corrections and, thus, paves the way for further improvements in theoretical predictions. Moreover, the difference between theory and experiment of $0.22 \pm 0.13_{\text{exp}}$ kHz, much smaller than the theoretical uncertainty (1.7 kHz) due to unknown higher-order QED corrections, indicates that these corrections are small and theoretical predictions after their calculations may indeed achieve a precision equal to or better than the experimental one of 0.13 kHz. Such calculations are feasible now, since the α^5Ry terms has been confirmed experimentally. Interestingly, the larger difference between the theoretical prediction and our experimental value for the 2^3P_1-2^3P_2 interval of 1.5 kHz indicates the significance of higher-order QED corrections due to singlet-triplet mixing of 2^1P_1 with 2^3P_1, which are very difficult to estimate. This shows that it would be much more difficult to achieve similar theoretical precision for this interval than for the larger one. The very good agreement for the 2^3P_0-2^3P_2 interval also opens up the possibility of studying fine-structure splitting in other elements, such as Li or Be, for which high-precision calculations based on QED theory are also feasible.

The authors thank Z.-T. Lu for helpful discussions and comments. This work is jointly supported by Chinese Academy of Science (Grant No. XDB21010400), and the Natural Science Foundation of China (Grants No. 11304303, No. 21225314, and No. 21688102).

*Corresponding author.
robert@mail.ustc.edu.cn
†Corresponding author.
smhu@ustc.edu.cn

[1] C. Schwartz, Phys. Rev. **134**, A1181 (1964).
[2] F. Ficek, D. F. J. Kimball, M. Kozlov, N. Leefer, S. Pustelny, and D. Budker, arXiv:1608.05779.
[3] T. Zhang, Z. C. Yan, and G. W. F. Drake, Phys. Rev. Lett. **77**, 1715 (1996).
[4] K. Pachucki and V. A. Yerokhin, Phys. Rev. A **80**, 019902(E) (2009).
[5] K. Pachucki and V. A. Yerokhin, Phys. Rev. Lett. **104**, 070403 (2010).
[6] D. Hanneke, S. Fogwell, and G. Gabrielse, Phys. Rev. Lett. **100**, 120801 (2008).
[7] R. Bouchendira, P. Clade, S. Guellati-Khelifa, F. Nez, and F. Biraben, Phys. Rev. Lett. **106**, 080801 (2011).
[8] G. P. Feng, X. Zheng, Y. R. Sun, and S. M. Hu, Phys. Rev. A **91**, 030502(R) (2015).
[9] J. Castillega, D. Livingston, A. Sanders, and D. Shiner, Phys. Rev. Lett. **84**, 4321 (2000).
[10] T. Zelevinsky, D. Farkas, and G. Gabrielse, Phys. Rev. Lett. **95**, 203001 (2005).
[11] J. S. Borbely, M. C. George, L. D. Lombardi, M. Weel, D. W. Fitzakerley, and E. A. Hessels, Phys. Rev. A **79**, 060503 (2009).
[12] A. Marsman, M. Horbatsch, and E. A. Hessels, J. Phys. Chem. Ref. Data **44**, 031207 (2015).
[13] M. C. George, L. D. Lombardi, and E. A. Hessels, Phys. Rev. Lett. **87**, 173002 (2001).
[14] M. Smiciklas and D. Shiner, Phys. Rev. Lett. **105**, 123001 (2010).
[15] G. P. Feng, Y. R. Sun, X. Zheng, and S. M. Hu, Acta Phys. Sin. **63**, 123201 (2014).
[16] C. F. Cheng, W. Jiang, G. M. Yang, Y. R. Sun, H. Pan, Y. Gao, A. W. Liu, and S. M. Hu, Rev. Sci. Instrum. **81**, 123106 (2010).
[17] Y. R. Sun, G. P. Feng, C. F. Cheng, L. Y. Tu, H. Pan, G. M. Yang, and S. M. Hu, Acta Phys. Sin. **63**, 170601 (2012).
[18] J. Alnis, A. Matveev, N. Kolachevsky, T. Udem, and T. W. Hänsch, Phys. Rev. A **77**, 053809 (2008).
[19] C. F. Cheng, Y. R. Sun, H. Pan, Y. Lu, X. F. Li, J. Wang, A. W. Liu, and S. M. Hu, Opt. Express **20**, 9956 (2012).
[20] Z. C. Yan and G. W. F. Drake, Phys. Rev. A **50**, R1980 (1994).
[21] A. Marsman, M. Horbatsch, and E. A. Hessels, Phys. Rev. A **86**, 040501 (2012).
[22] C. J. Sansonetti, C. E. Simien, J. D. Gillaspy, J. N. Tan, S. M. Brewer, R. C. Brown, S. Wu, and J. V. Porto, Phys. Rev. Lett. **107**, 023001 (2011).
[23] R. C. Brown, S. Wu, J. V. Porto, C. J. Sansonetti, C. E. Simien, S. M. Brewer, J. N. Tan, and J. D. Gillaspy, Phys. Rev. A **87**, 032504 (2013).
[24] M. Kleinert, M. E. G. Dahl, and S. Bergeson, Phys. Rev. A **94**, 052511 (2016).